

Mixed mode fracture assessment of U-notched graphite Brazilian disk specimens by means of the local energy

A.R. Torabi*¹ and F. Berto^{2a}

¹Fracture Research Laboratory, Faculty of New Science and Technologies, University of Tehran,
P.O. Box 13741-4395, Tehran, Iran

²Department of Management and Engineering, University of Padova,
Stradella, S. Nicola 3-36100 Vicenza, Italy

(Received January 14, 2014, Revised March 1, 2014, Accepted March 5, 2014)

Abstract. A fracture criterion based on the strain energy density (SED) over a control volume, which embraces the notch edge, is employed in the present paper to assess the fracture loads of some U-notched Brazilian disk (UNBD) specimens. The specimens are made of commercial graphite and have been tested under pure mode I, pure mode II and mixed mode I/II loading. The results show that the SED criterion allows to successfully assess the fracture loads of graphite specimens for different notch tip radii and various mode mixity conditions with discrepancies that fall inside the scatter band of $\pm 20\%$.

Keywords: Strain Energy Density (SED); U-notch; brittle fracture; mixed mode loading; graphite; U-Notched Brazilian disk (UNBD)

1. Introduction

Graphite is generally used in a wide range of applications in different industrial fields such as aerospace, chemical, nuclear and steel-making industries etc. The main applications are thermal, chemical, electrical and mechanical. Dealing with aerospace industries, graphite is utilized for very specific aims, as for instance to protect metallic parts from aerodynamic heating. Dealing with electrical applications, carbon brushes in electric motors are generally made of graphite. Thrust bearings, journal bearings, piston rings and vanes, seals in shafts and fuel pumps of jet aero-engines are other examples in which graphite is widely employed due to a good combination of mechanical and auto-lubricant properties.

In the presence of stress concentrators like notches, the risk of nucleating cracks from notch border drastically increases. As an example, notches introduced in graphite components for joining thermally protective components to the main metallic or composite parts of the engineering structures should be mentioned.

The fracture behavior of cracked components made of brittle and quasi-brittle graphite materials have been investigated since 1970 considering different loading conditions and various

*Corresponding author, Ph.D., E-mail: a_torabi@ut.ac.ir

^aPh.D., E-mail: berto@gest.unipd.it

temperatures (see Lomakin *et al.* 1975, Sato *et al.* 1981, Yamauchi *et al.* 2001, Etter *et al.* 2004, Bruno and Latella 2006, Shi *et al.* 2008, Ayatollahi and Aliha 2008, Mostafavi *et al.* 2012, 2013, Nakhodchi *et al.* 2013).

Dealing with notched graphite components, only few researchers have faced the problem of the notch sensitivity of different kind of commercial graphite materials (Bazaj and Cox 1969, Kawakami 1985). More recently, Ayatollahi and Torabi systematically investigated the fracture behavior of V-notched graphite components under mode I loading conditions and different geometrical configurations. The notch apparent fracture toughness has been measured and the experimental values have been successfully assessed by using the mean stress (MS) model (Ayatollahi and Torabi 2010a). Fracture tests have been carried out also on V-notched Brazilian disk (V-BD) specimens weakened by V-shaped notches under mixed mode I/II and pure mode II loading (Ayatollahi and Torabi 2011). The fracture loads have been assessed by means of the generalized maximum tangential stress (V-MTS) criterion (Ayatollahi and Torabi 2011) and the strain energy density (SED) fracture criterion (Ayatollahi *et al.* 2011a). Dealing with torsion loading, a large bulk of experiments have been performed on round bars of polycrystalline isostatic graphite weakened by sharp and rounded-tip V-notches. The results have been predicted by means of the SED criterion (Berto *et al.* 2012a). Another recent investigation deals with brittle fracture of U-notched graphite materials under mixed mode loading (Berto *et al.* 2012b). The SED failure model has also been utilized to predict successfully the experimental fracture loads (Berto *et al.* 2012b) whereas by Torabi (2013a, b), other stress based criteria have been employed to predict the mode I experimental results taken from Berto *et al.* (2012b). A new set of experimental results have been provided by Torabi *et al.* (2013a) summarizing data from U-notched Brazilian disks (UNBD) made of polycrystalline graphite under pure mode I loading.

As repaired U-notches, by removing a short crack initiated from the U-notch border, key-hole notches have attracted interest in the context of brittle fracture of notches. In this area, a recent work has been performed on isostatic graphite plates containing a central slit with two key-hole ends under mixed mode I/II loading conditions (Lazzarin *et al.* 2013). The failure theory has been the SED criterion capable of predicting successfully the experimentally obtained fracture loads (Lazzarin *et al.* 2013). By considering V-notches with end holes, a large bulk of tests has been performed under pure compression (Berto *et al.* 2013).

Dealing with pure mode II fracture in graphite materials weakened by U-shaped notches, a research paper has been more recently published (Torabi *et al.* 2013b) in which the experimentally obtained mode II fracture toughness and the fracture initiation angle of U-notched Brazilian disk (UNBD) specimens made of coarse-grained polycrystalline graphite have been well predicted by means of two failure criteria namely the U-notched maximum tangential stress (UMTS) and the U-notched mean stress (UMS). The same criteria have been applied for the fracture assessment of U-notched Brazilian disk (UNBD) specimens under mixed mode loadings (Torabi *et al.* 2013c).

The main goal of the present work is to verify the suitability of the SED criterion in predicting the experimental fracture loads of some recent UNBD graphite specimens made of the same material under pure mode I, pure mode II, mixed mode loading taken from Torabi *et al.* (2013a, b, c). A comparison between the experimental and theoretical results reveals that the fracture loads can be successfully predicted by means of the SED criterion with discrepancies that fall inside the scatter band of $\pm 20\%$. This research confirms that the SED criterion is effective in predicting brittle fracture of notched graphite components under mixed mode I/II loading conditions. Moreover, the choice of maintaining, as first engineering approximation, the same control volume in the case of mode I and mode II loadings is well confirmed in the present contribution.

Table 1 Properties of the tested graphite material (Torabi *et al.* 2013a)

Material property	Value
Elastic modulus, E (GPa)	8.05
Poisson's ratio	0.2
Ultimate tensile strength (MPa)	27.5
Plane-strain fracture toughness ($\text{MPa m}^{0.5}$)	1.0
Bulk density (kg/m^3)	1710
Mean grain size (μm)	320
Porosity (%)	9

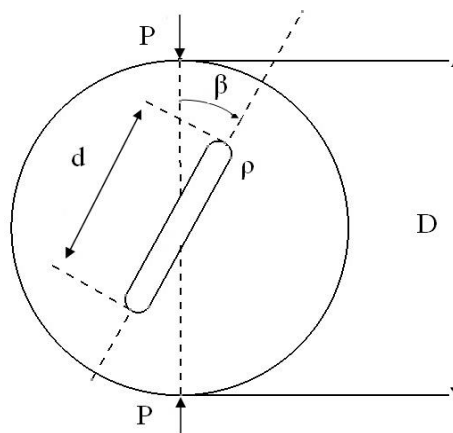


Fig. 1 The UNBD specimen

2. Experimental results reported in the literature

2.1 Material

In Torabi *et al.* (2013a, b, c), a type of commercial coarse-grain polycrystalline graphite has been utilized in fracture experiments with the properties presented in Table 1.

2.2 Specimen

The specimen used for conducting the fracture tests was the well-known Brazilian disk (BD) specimen containing a central bean-shaped slit with two U-shaped ends. This specimen (Fig. 1), called the U-notched BD (UNBD), has been initially proposed by Ayatollahi and Torabi (2010b) and used to measure the mode II notch fracture toughness of U-shaped notches in PMMA and soda-lime glass. The elastic stress distribution around U-shaped notches in the UNBD specimen has been analyzed by Torabi and Jafarinezhad (2012) and a wide range of notch shape factors has been presented. Note that this disk-type specimen which contained a central sharp crack (its original form) has been proposed in the past and frequently utilized by the researchers for investigating brittle fracture under mode I, mixed mode I/II and also pure mode II loading conditions (see for example Sato *et al.* 1981, Yamauchi *et al.* 2001, Ayatollahi and Aliha 2008).

In Fig. 1, β is the angle between the loading direction and the notch bisector line. The parameters D and P denote the disk diameter and the applied compressive load, respectively. When the direction of the applied load P is along the notch bisector line (i.e., $\beta=0$), the central notch is subjected to pure mode I loading conditions. When β enhances gradually from zero, the loading condition varies from pure mode I towards pure mode II. For a particular angle, called β_{II} , pure mode II deformation is obtained. The angle β_{II} is always less than 90° and depends upon the notch length and the notch tip radius. This angle can be determined by using the finite element (FE) method as was presented by Torabi and Jafarinezhad (2012).

The diameter D , the overall notch length d (i.e., the tip-to-tip distance) and the thickness of the UNBD specimens were 60 mm, 18 mm and 10 mm, respectively. The notch tip radii (ρ) were equal to 0.5, 1, 2 and 4 mm. To fabricate the specimens, first, a graphite block was provided. Then, three slices of 10 mm thick were cut from the block by using a cutter blade. The geometry of each sample was given to a high-precision 2-D CNC water jet cutting machine and finally, the UNBD specimens were fabricated. Before performing the fracture tests, the specimens were polished by using a fine abrasive paper in order to remove possible local stress raisers remained from the manufacturing process. Fig. 2 displays the UNBD graphite specimens fabricated (not polished).

To perform fracture tests under mixed mode loading conditions, the angle β_{II} should first be determined so that we could select appropriate intermediate angles between $\beta=0$ (pure mode I) and $\beta=\beta_{II}$ (pure mode II). The values of β_{II} for different values of the relative notch length (RNL) and the relative notch tip radius (RNR) have been presented by Torabi and Jafarinezhad (2012) for the UNBD specimen. Considering the RNL (i.e., the ratio of the overall notch length to disc diameter) equal to 0.3 for the specimens, β_{II} angles can be obtained from Torabi and Jafarinezhad (2012) to be the values in the range of 31 to 33 (deg.) for different notch tip radii. Therefore, the angles $\beta=0$, 10, 20, 30 (deg.) were selected for pure mode I, mixed mode I/II and pure mode II fracture tests. For each notch tip radius, twelve tests were carried out (four for each value of β) under displacement-control conditions with a loading rate of 0.1 mm/min; the fracture load of each sample was finally recorded. 48 test results were totally provided under pure mode I, mixed mode I/II and pure mode II loading conditions. Figs. 3 and 4 show the UNBD graphite specimens during mode I and mixed mode I/II tests, respectively.



Fig. 2 The UNBD graphite specimens fabricated (not polished)



Fig. 3 The UNBD graphite specimen during mode I fracture test

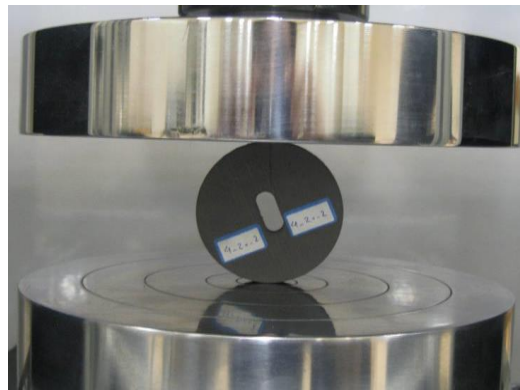


Fig. 4 The UNBD graphite specimen during mixed mode I/II fracture test tested for $\beta=10^\circ$

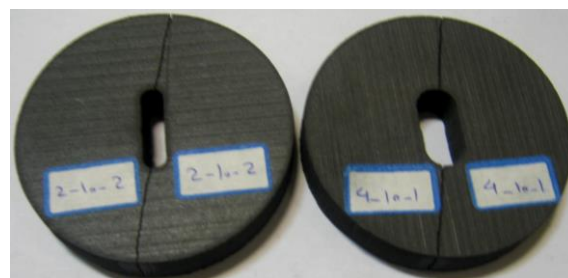


Fig. 5 The broken UNBD specimens

Two broken specimens are shown in Fig. 5.

The experimentally recorded fracture loads for UNBD graphite specimens are presented in Table 2 as taken from the original references (Torabi *et al.* 2013a, b, c). The load-displacement graphs recorded from the tests were completely linear up to final fracture and the fracture for each specimen was seen to occur suddenly. Thus, brittle fracture criteria based on the linear elastic

Table 2 The experimentally recorded fracture loads for UNBD graphite specimens (Torabi *et al.* 2013a-c) P_1 , P_2 and P_3 are the repeated tests for each configuration

β (deg.)	ρ (mm)	P_1 (N)	P_2 (N)	P_3 (N)	$P_{av.}$ (N)
0	0.5	4164	4267	4040	4157
0	1	4410	4561	4830	4600
0	2	4228	4448	4382	4353
0	4	4000	4188	3722	3970
10	0.5	4101	3836	4203	4047
10	1	4526	4409	4400	4445
10	2	4040	4024	4049	4038
10	4	3634	3551	3540	3575
20	0.5	3983	3599	3947	3843
20	1	3880	3959	4049	3963
20	2	4036	4018	3710	3921
20	4	3678	3398	3000	3359
30	0.5	3120	3210	3439	3256
30	1	3520	3466	3499	3495
30	2	3700	3857	3378	3645
30	4	3519	3620	3369	3502

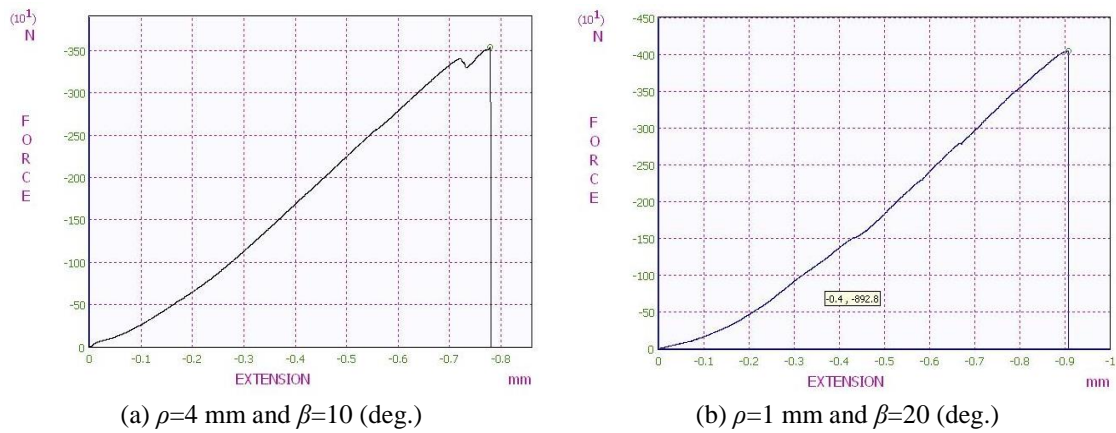


Fig. 6 Two sample load-displacement curves for the graphite UNBD specimens

fracture mechanics (LEFM) can be applied. Fig. 6 displays two sample load-displacement curves for the graphite UNBD specimens.

In the next section, a brittle fracture model is described and formulated with the aim to estimate the experimental results.

3. Brittle fracture model based on the Strain Energy Density over a control volume

The most critical issue for designers is the existence of appropriate fracture criteria to assess the behavior at failure of graphite components weakened by sharp and blunt notches. With the aim to

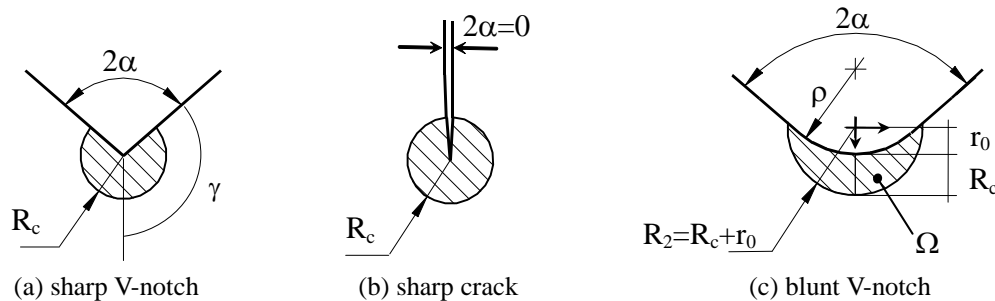


Fig. 7 Control volume (area) for sharp V-notch (a), sharp crack (b) and blunt V-notch (c) under mode I loading. Distance $r_0 = \rho \times (\pi - 2\alpha) / (2\pi - 2\alpha)$. For a U-notch $r_0 = \rho / 2$

provide a suitable criterion, a strain-energy-density based criterion is proposed and applied in this section. As will be seen in the following part of the manuscript, the experimental fracture loads of UNBD graphite specimens, described in Table 2, can be estimated with an acceptable accuracy. Sih (1974) defined the strain energy density factor S as the product of the strain energy density at a certain distance from the crack tip. Fracture was thought to be controlled by a critical value of S , named S_c , which is a material property. The crack growth direction can be determined by imposing a minimum condition on the factor S . This condition permits to determine the direction where the crack can propagate more easily inside the material. Along that line, in fact, the strain energy required for propagation reaches a minimum. The Sih's model is a point-wise criterion while the averaged strain energy density criterion (SED), proposed by Lazzarin and Zambardi (2001), Lazzarin and Berto (2005), Berto and Lazzarin (2009) states that fracture should occur when the mean value of the strain energy density over a known control volume is equal to a critical value W_c , which depends on the material. This critical value is independent of the notch geometry and in particular on the notch acuity and permits to summarize all of the data from very different geometries in the same narrow scatter band. In the case of brittle or quasi-brittle materials subjected to static and monotonic loads, the control volume is thought as dependent on the ultimate tensile strength and the fracture toughness K_{Ic} . This idea is reminiscent of Neuber's concept of elementary structural volume (Neuber 1958, Berto *et al.* 2008, 2009, Berto and Lazzarin 2010, Berto and Zappalorto 2011, 2012, Berto 2012, Radaj *et al.* 2009a, b, Radaj *et al.* 2013). The averaged strain energy density criterion was first formalized and applied to sharp V-notches under mode I and mixed I/II loading (Lazzarin and Zambardi 2001) and later extended to blunt U and V-notches (Lazzarin and Berto 2005, Berto and Lazzarin 2009). For a crack, the critical volume is a circle of radius R_c centered at the crack tip (Fig. 7(b)). Under plane-strain conditions, the critical length, R_c , can be evaluated by the following expression (Yosibash *et al.* 2004)

$$R_c = \frac{(1 + \nu)(5 - 8\nu)}{4\pi} \left(\frac{K_{Ic}}{\sigma_t} \right)^2 \quad (1)$$

In Eq. (1), K_{Ic} is the fracture toughness, ν the Poisson's ratio and σ_t the ultimate tensile strength of material. Dealing with sharp V-notches, the critical volume assumes the shape of circular sector of radius R_c centered at the notch tip (Fig. 7(a)) while for a blunt V-notch under mode I loading, the volume assumes the crescent-moon shape depicted in Fig. 7(c). In this last case, R_c is the depth

measured along the notch bisector line. The external radius of the crescent shape is equal to $R_c + r_0$, being r_0 the distance between the notch tip and the origin of the local coordinate system (see Fig. 7). Such a distance depends on the V-notch opening angle 2α , according to the expression $r_0 = \rho \times (\pi - 2\alpha) / (2\pi - 2\alpha)$ (Lazzarin and Berto 2005, Berto and Lazzarin 2009).

Under mixed mode loading, the critical volume is no longer centered on the notch tip, but rather on the point where the principal stress reaches its maximum value along the border of the notch. It was fundamentally assumed that the crescent shape volume rotates rigidly under mixed mode, with no change in shape and size (see Fig. 8). This is the governing idea of the ‘*equivalent local mode I*’ approach, as suggested and applied to U and V-notches (Gomez *et al.* 2007, Lazzarin *et al.* 2009).

Under mode I loading when the area embraces the semicircular edge of the notch (and not its rectilinear flanks), the mean value of SED can be expressed in the following form (Lazzarin and Berto 2005)

$$\bar{W}_1 = F(2\alpha) \times H(2\alpha, \frac{R_c}{\rho}) \times \frac{\sigma_{\text{tip}}^2}{E} \quad (2)$$

where $F(2\alpha)$ depends on previously defined parameters as follows

$$F(2\alpha) = \left(\frac{q-1}{q} \right)^{2(1-\lambda_1)} \left[\frac{\sqrt{2\pi}}{1+\tilde{\omega}_1} \right]^2 \quad (3)$$

which are reported in the last column of Table 3. H is summarized for U-notches in Table 4 as a function of the ratio R_c/ρ and for different values of the Poisson’s ratio.

Table 3 Parameters of the stress distributions

2α [rad]	q	λ_1	$\tilde{\omega}_1$	$F(2\alpha)$
0	2.0000	0.5	1	0.7850
$\pi/6$	1.8333	0.5014	1.034	0.6917
$\pi/4$	1.7500	0.5050	1.014	0.6692
$3\pi/4$	1.2500	0.6736	0.432	1.0717

Table 4 H values for U-notched specimens

R_c/ρ	H				
	$\nu=0.1$	$\nu=0.15$	$\nu=0.2$	$\nu=0.25$	$\nu=0.3$
0.0005	0.6294	0.6215	0.6104	0.5960	0.5785
0.001	0.6286	0.6207	0.6095	0.5952	0.5777
0.005	0.6225	0.6145	0.6033	0.5889	0.5714
0.01	0.6149	0.6068	0.5956	0.5813	0.5638
0.05	0.5599	0.5515	0.5401	0.5258	0.5086
0.1	0.5028	0.4942	0.4828	0.4687	0.4518
0.3	0.3528	0.3445	0.3341	0.3216	0.3069
0.5	0.2672	0.2599	0.2508	0.2401	0.2276
1	0.1590	0.1537	0.1473	0.1399	0.1314

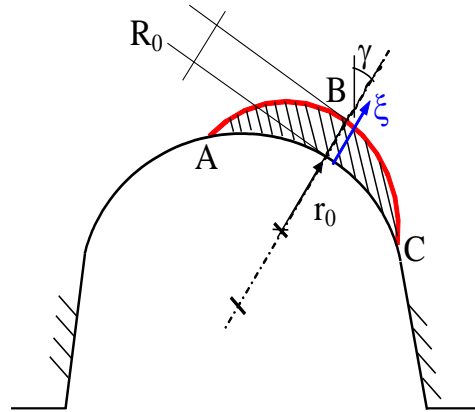


Fig. 8 Critical volume for blunt notches under mixed mode loading

The expression for U-notches under mixed mode is analogous to that valid for notches in mode I only updating σ_{iip} with σ_{\max} which is the maximum principal stress along the notch edge outside the notch bisector line as widely discussed and motivated by Gomez *et al.* (2007), Lazzarin *et al.* (2009), Berto and Lazzarin (2014)

$$\overline{W}^{(e)} = H^* \left(2\alpha, \frac{R_c}{\rho} \right) \times \frac{\pi \sigma_{\max}^2}{4E} \quad (4)$$

where H^* depends again on the normalized radius R_c/ρ , the Poisson's ratio ν and the loading conditions. For different configurations of mode mixity, the function H , analytically obtained under mode I loading, was shown to be very close to H^* (Gomez *et al.* 2007, Lazzarin *et al.* 2009, Berto and Lazzarin 2014). This idea of equivalent local mode I was first discussed by Gomez *et al.* (2007). In fact, under mixed mode loading, the line normal to the notch edge (direction ζ in Fig. 8) starting from the point of maximum principal stress behaves as a virtual bisector line under pure mode I, being the stress distribution along that line almost coincident with that obtained along the notch bisector under mode I loading (Gomez *et al.* 2007, Lazzarin *et al.* 2009, Berto and Lazzarin 2014).

A good alternative, avoiding any simplifying assumption, is to derive the SED values directly from finite element (FE) models without using any equation based on stress based parameters. The advantage of the direct evaluation of the SED from a FE model is that the value of this parameter is mesh-independent as described by Lazzarin *et al.* (2008, 2010). A very coarse mesh can be adopted for the SED evaluation contrary to the mesh required to evaluate the notch stress intensity factors or other stress based parameters. A recent application of the SED approach dealing with high temperature fatigue tests (Berto *et al.* 2013) takes advantage of this very convenient property. The SED is also able to take into account the three-dimensional effects due to a finite thickness of the plate as described by Harding *et al.* (2010), Kotousov *et al.* (2010), Berto *et al.* (2011, 2012c).

4. SED approach for fracture analysis of UNBD graphite specimens

The fracture criterion described in the previous section is employed here to predict the fracture

loads obtained from the experiments performed on the UNBD graphite specimens. In order to compute the SED values under mixed mode and mode II loading, first a finite element model was created for each graphite specimen. A typical mesh used in the numerical analyzes is shown in Fig. 9(a). The averaged strain energy density criterion (SED) states that brittle fracture occurs when the mean value of the strain energy density over a control volume, \bar{W} , is equal to a critical value W_c , which depends on the material but not on notch geometry (Lazzarin and Zambardi 2001). The concept of strain energy density has been reported in the literature in order to predict the fatigue behavior of notches, first under uniaxial and multi-axial stresses (see Glinka 1985, Glinka *et al.* 1995). In these papers, however, the fatigue behavior of the components was thought of as fully controlled by stresses at the notch tip and the criterion cannot be directly extended to small notch radii and to pointed V-notches.

This critical value can be determined from the ultimate tensile strength σ_t according to Beltrami's expression

$$W_c = \frac{\sigma_t^2}{2E} \quad (5)$$

In parallel, the control volume definition via the control radius R_c requires the knowledge of the fracture toughness K_{Ic} and the Poisson's ratio ν , see Eq. (1). The critical load that is sustainable by a notched component can be predicted by imposing \bar{W} equal to the critical value W_c . This value is considered here as constant under mode I, mode II and in-plane mixed mode conditions. This assumption has been extensively verified for a number of different brittle and quasi-brittle materials (Lazzarin and Zambardi 2001, Lazzarin and Berto 2005, Berto and Lazzarin 2009 2013).

As presented in Table 1, the properties of the graphite material used by Torabi *et al.* (2013a, b, c) are: $\sigma_t=27.5$ MPa, $K_{Ic} = 1 \text{ MPa}\sqrt{\text{m}}$, Poisson's ratio $\nu=0.2$. As a result, the critical SED for the reported graphite material is $W_c = 0.0469 \text{ MJ/m}^3$ whereas the radius of the control volume is $R_c = 0.429$ mm considering realistic plane-strain conditions as made by Ayatollahi *et al.* (2011a) for the same commercial material.

The SED occurring inside the control volume embracing the edges of U-notches has been calculated numerically by using the FE code ANSYS. For each geometry, a model was created by considering that it requires an accurate definition of the control volume where the strain energy

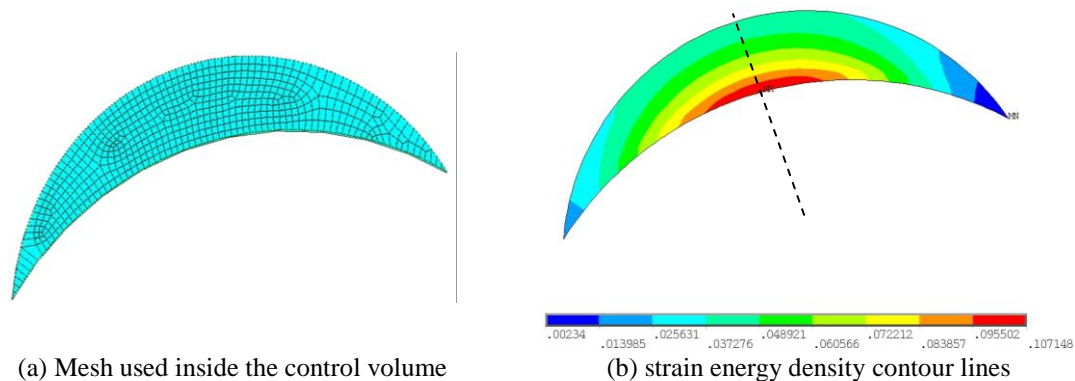


Fig. 9 Mesh used inside the control volume and strain energy density contour lines (b); case $\rho=0.5$ mm

density should be averaged (see Fig. 9(b)). The entire analyzes were performed by using eight-node elements under plane-strain conditions.

Fig. 9 refers to the case $\rho=0.5$ mm and $\beta=30^\circ$, which corresponds to pure mode II loading. The strain energy density contour lines inside the control volume are shown in Fig. 9(b). Notice that the SED is not symmetric with respect to the notch bisector line because of the presence of pure shear deformation, but it is almost symmetric with respect to a virtual line normal to the notch edge and dividing in two parts the control volume.

Table 5 summarizes the outlines of the experimental, numerical and theoretical findings for UNBD graphite specimens with four different notch tip radii ($\rho= 0.5, 1, 2, 4$ mm) reported in literature and re-analyzed by means of SED. Particularly, Table 5 summarizes the experimental loads to fracture (P) for each value of the notch radius ρ compared with the theoretical values (P_{th}) based on the SED evaluation. P_{th} is the theoretical load obtained by keeping a constant averaged energy equal to 0.0469 MJ/m³ over the control volume. For deriving P_{th} , it is important to remember that the load is proportional to the square root of the strain energy density under linear elastic conditions. \bar{W} can be evaluated by using Eq. (4) or more conveniently directly by numerical models and using a coarse free mesh.

Table 5 Synthesis based on SED

Notch radius [mm]	Loading angle β [°]	\bar{W} [MJ/m ³]	Theoretical fracture load P_{th} [N]	Experimental fracture load P [N]	$\sqrt{(\bar{W}/W_c)}$	$\Delta(P-P_{th})/P$ (%)
0.5	0	0.0421	4396	4164	0.947	-5.6
0.5	0	0.0442	4396	4267	0.971	-3.0
0.5	0	0.0396	4396	4040	0.919	-8.8
1	0	0.0474	4386	4410	1.006	0.5
1	0	0.0507	4386	4561	1.040	3.8
1	0	0.0569	4386	4830	1.101	9.2
2	0	0.0509	4059	4228	1.042	4.0
2	0	0.0563	4059	4448	1.096	8.7
2	0	0.0546	4059	4382	1.079	7.4
4	0	0.0552	3688	4000	1.085	7.8
4	0	0.0605	3688	4188	1.136	11.9
4	0	0.0478	3688	3722	1.009	0.9
0.5	10	0.0557	3764	4101	1.090	8.2
0.5	10	0.0487	3764	3836	1.019	1.9
0.5	10	0.0585	3764	4203	1.117	10.4
1	10	0.0549	4182	4526	1.082	7.6
1	10	0.0521	4182	4409	1.054	5.1
1	10	0.0519	4182	4400	1.052	4.9
2	10	0.0485	3974	4040	1.017	1.6
2	10	0.0481	3974	4024	1.013	1.3
2	10	0.0487	3974	4049	1.019	1.9
4	10	0.0462	3663	3634	0.992	-0.8
4	10	0.0441	3663	3551	0.970	-3.1
4	10	0.0438	3663	3540	0.967	-3.5
0.5	20	0.0767	3115	3983	1.278	21.8

Table 5 Continued

1	20	0.0509	3724	3880	1.042	4.0
1	20	0.0530	3724	3959	1.063	5.9
1	20	0.0555	3724	4049	1.087	8.0
2	20	0.0550	3728	4036	1.083	7.6
2	20	0.0545	3728	4018	1.078	7.2
2	20	0.0465	3728	3710	0.995	-0.5
4	20	0.0494	3583	3678	1.026	2.6
4	20	0.0422	3583	3398	0.948	-5.4
4	20	0.0329	3583	3000	0.837	-19.4
0.5	30	0.0637	2678	3120	1.165	14.2
0.5	30	0.0674	2678	3210	1.199	16.6
0.5	30	0.0774	2678	3439	1.284	22.1
1	30	0.0523	3334	3520	1.056	5.3
1	30	0.0507	3334	3466	1.040	3.8
1	30	0.0517	3334	3499	1.049	4.7
2	30	0.0534	3466	3700	1.067	6.3
2	30	0.0581	3466	3857	1.113	10.1
2	30	0.0445	3466	3378	0.974	-2.6
4	30	0.0477	3488	3519	1.009	0.9
4	30	0.0505	3488	3620	1.038	3.7
4	30	0.0438	3488	3369	0.966	-3.5

The sixth column of Table 5 presents the relative deviation between the mean values of the experimental fracture loads and the theoretical ones evaluated by means of SED. It is clearly seen in Table 5 that except for the notch radius of 0.5 mm, the discrepancies are less than 20% (and in the majority of the cases less than 10%) demonstrating the effectiveness of the SED criterion under mixed mode loading conditions. The discrepancy for $\rho=0.5$ mm and prevalent mode II was found to be a bit higher and averagely equal to 17.5% with some peaks reaching 22%. This moderate agreement may or may not be attributed to possible inaccuracy in the experiments of Torabi *et al.* (2013b) due to some manufacturing problems for the specimens with small notch radii.

As discussed by Torabi and Berto (2013), another possible reason for this discrepancy could be the issue commonly called geometry effect in mixed mode I/II fracture of brittle materials that can be relevant for smaller notch tip radii close to the crack case (see Ayatollahi and Aliha 2005, 2006, 2011, Smith *et al.* 2001, Ayatollahi *et al.* 2011b, Ayatollahi and Pirmohammad 2013, Aliha *et al.* 2012). Other interesting features under fatigue loading are discussed by Brighenti (2008) and Carpinteri *et al.* (2010a, b) dealing with different materials while wide reviews on cracks initiated in structural components weakened by notches are reported by Brighenti (2008), Carpinteri *et al.* (2010a, b, 2013) and Brighenti and Carpinteri (2013). As visible from Table 5 which reports the relative deviation between the experimental and the theoretically predicted values, the accuracy in fracture load assessment does not change varying the angle β and it is sound also in the case of prevalent mode II loading. The only exception is the case $\rho=0.5$ mm, discussed above.

The results are given also in graphical form in Fig. 10 (a), (b), (c), (d) where the *experimental* values of the fracture loads (open dots) have been compared with the *theoretical* predictions based on the constancy of the SED in the control volume (solid line). The plots are given for the UNBD

graphite specimens as a function of the notch radius ρ . The trend of the theoretically estimated loads is in good agreement with the experimental ones.

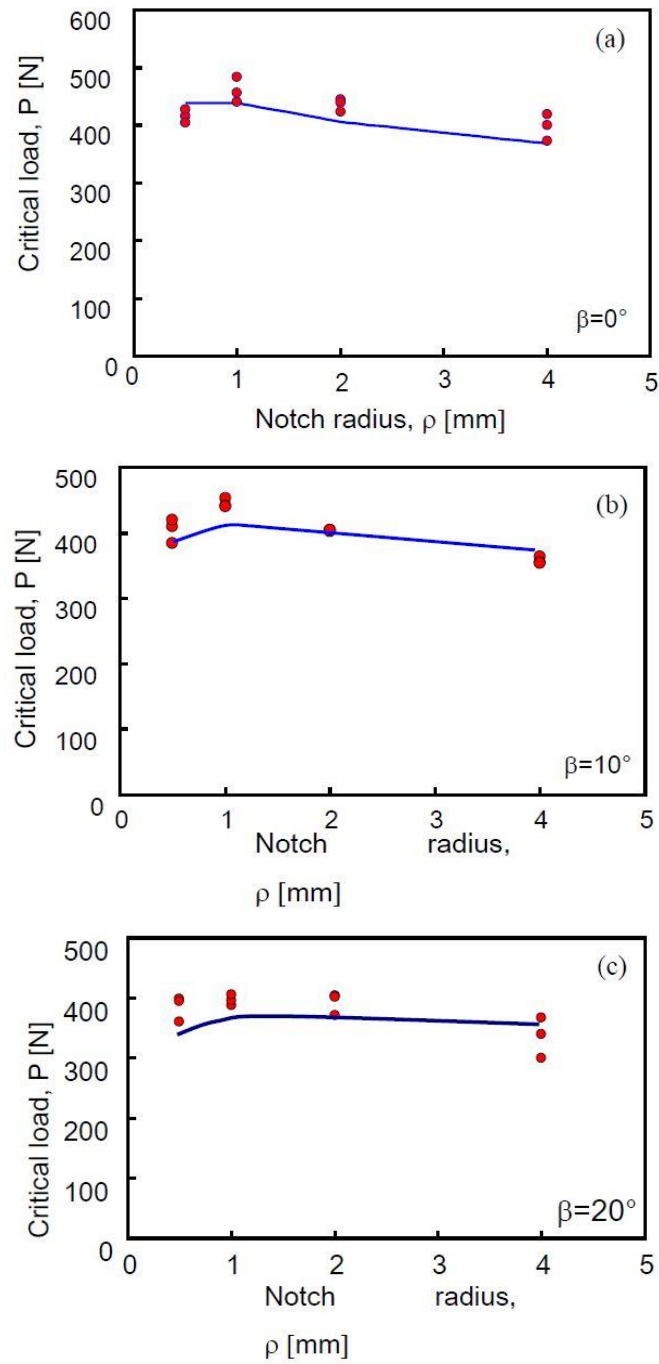


Fig. 10 Fracture prediction based on SED; (a) pure mode I ($\beta=0^\circ$); (b) $\beta=10^\circ$; (c) $\beta=20^\circ$; (d) $\beta=30^\circ$

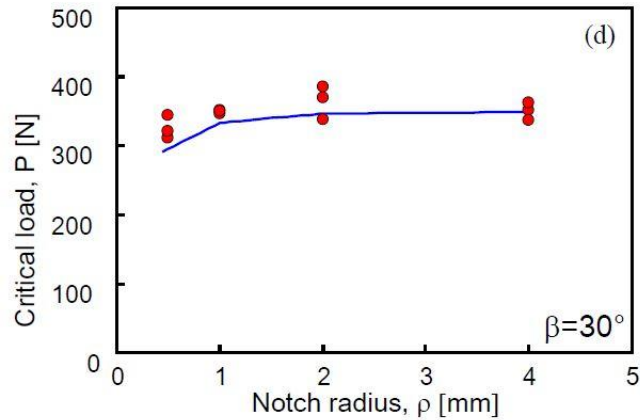


Fig. 10 Continued

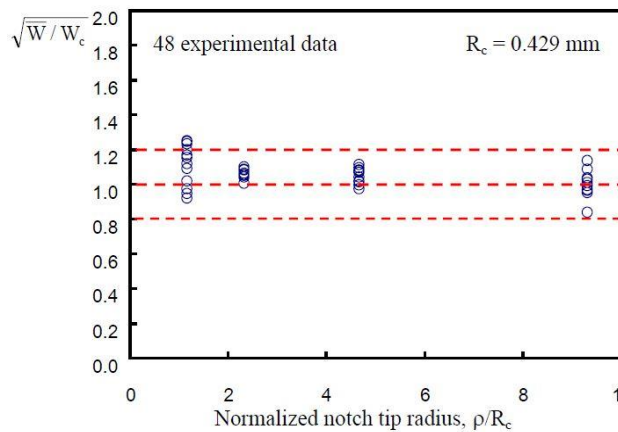


Fig. 11 Synthesis of brittle fracture data from UNBD graphite specimens

A synthesis in terms of the square root value of the local energy averaged over the control volume (of radius R_c), normalized with respect to the critical energy of the material as a function of the notch tip radius is shown in Fig. 11. The plotted parameter is proportional to the fracture load. The goal is to study the influence of the notch tip radius on the fracture prediction based on SED. From the figure, it is obvious that all of the values fall inside a scatter ranging from 0.80 to 1.20 with the majority of the data inside 0.90 to 1.10 and only few exceptions outside that range. The synthesis confirms also the choice of the control volume which seems to be suitable to characterize the material behavior under different loading conditions, ranging from pure mode I to pure mode II loading, and different geometrical configurations. The scatter of the experimental data presented here is in very good agreement with the recent database in terms of SED reported by Berto and Iazzarini (2009, 2013) for similar materials. Finally, for completeness, Table 6 summarizes the comparison between SED fracture assessment and the predictions made by using the U-notched maximum tangential stress (UMTS) criterion and the U-notched mean stress (UMS) criterion (Torabi 2013a, b, c).

Table 6 Comparison between SED and other criteria (Torabi *et al.* 2013a, b c); U-notched maximum tangential stress (UMTS) criterion and U-notched mean stress (UMS) criterion

Notch radius	Loading angle β	Exp. fracture load	Th. fracture load SED	Th. fracture load UMTS	Th. fracture load UMS
[mm]	[°]	P_{av} [N]	$P_{th, SED}$ [N]	$P_{th, UMTS}$ [N]	$P_{th, UMS}$ [N]
0.5	0	4157	4396	3583	4257
1	0	4600	4386	3515	4163
2	0	4353	4059	3818	4296
4	0	3970	3688	3938	4322
0.5	10	4047	3764	3683	3804
1	10	4445	4182	4090	4134
2	10	4038	3974	3796	3796
4	10	3575	3663	3503	3503
0.5	20	3843	3115	3343	3459
1	20	3963	3724	3725	3844
2	20	3921	3728	3529	3568
4	20	3359	3583	3090	3090
0.5	30	3256	2678	2774	2947
1	30	3495	3334	3065	3223
2	30	3645	3466	3426	3536
4	30	3502	3488	3698	3737

5. Conclusions

A criterion based on the local energy averaged over a control volume was utilized in the present research to predict the experimentally recorded fracture loads of a new complete set of experimental data taken from the literature and dealing with graphite Brazilian disks weakened by U-notches and subjected to mixed mode (I+II) loadings. A good accuracy was found for the SED model considering the variability of geometrical parameters and loading conditions involved in the synthesis. The choice of a constant size of the control volume is confirmed to be a sound engineering approximation at least for the case of in-plane mixed mode loading.

References

- Aliha, M.R.M., Heidari-Rarani, M., Shokrieh, M.M. and Ayatollahi, M.R. (2012), "Experimental determination of tensile strength and K_{Ic} of polymer concretes using semi-circular bend (SCB) specimens", *Struct. Eng. Mech.*, **43**(6), 823-833.
- Ayatollahi, M.R. and Aliha, M.R.M. (2008), "Mixed mode fracture analysis of polycrystalline graphite-A modified MTS criterion", *Carbon*, **46**, 1302-1308.
- Ayatollahi, M.R. and Aliha, M.R.M. (2005), "Cracked Brazilian disc specimen subjected to mode II deformation", *Eng. Fract. Mech.*, **72**, 493-503.
- Ayatollahi, M.R. and Aliha, M.R.M. (2006), "On determination of mode II fracture toughness using semi-circular bend specimen", *Int. J. Solids Struct.*, **43**, 5217-5227.
- Ayatollahi, M.R. and Aliha, M.R.M. (2011), "On the use of anti-symmetric four-point bend specimen for mode II fracture experiments", *Fat. Fract. Eng. Mater. Struct.*, **34**, 898-907.
- Ayatollahi, M.R., Aliha, M.R.M. and Saghafi, H. (2011b), "An improved semi-circular bend specimen for investigating mixed mode brittle fracture", *Eng. Fract. Mech.*, **78**, 110-123.

- Ayatollahi, M.R., Berto, F. and Lazzarin, P. (2011a), "Mixed mode brittle fracture of sharp and blunt V-notches in polycrystalline graphite", *Carbon*, **49**, 2465-2474.
- Ayatollahi, M.R. and Pirmohammad, S. (2013), "Temperature effects on brittle fracture in cracked asphalt concretes", *Struct. Eng. Mech.*, **45**(1), 19-32.
- Ayatollahi, M.R. and Torabi, A.R. (2011), "Failure assessment of notched polycrystalline graphite under tensile-shear loading", *Mater. Sci. Eng. A*, **528**, 5685-5695.
- Ayatollahi, M.R. and Torabi, A.R. (2010a), "Tensile fracture in notched polycrystalline graphite specimens", *Carbon*, **48**, 2255-2265.
- Ayatollahi, M.R. and Torabi, A.R. (2010b), "Determination of mode II fracture toughness for U-shaped notches using Brazilian disc specimen", *Int. J. Solids Struct.*, **47**, 454-465.
- Bazaj, D.K. and Cox, E.E. (1969), "Stress concentration factors and notch sensitivity of graphite", *Carbon*, **7**(6), 689-697.
- Berto, F., Lazzarin, P. and Radaj, D. (2008), "Fictitious notch rounding concept applied to sharp V-notches: Evaluation of the microstructural support factor. Part I: Basic stress equations", *Eng. Fract. Mech.*, **75**, 3060-3072.
- Berto, F., Lazzarin, P. and Radaj, D. (2009), "Fictitious notch rounding concept applied to sharp V-notches: evaluation of the microstructural support factor for different failure hypotheses. Part II: Microstructural support analysis", *Eng. Fract. Mech.*, **76**, 1151-1175.
- Berto, F. and Lazzarin, P. (2009), "A Review of the volume-based strain energy density approach applied to V-notches and welded structures", *Theor. Appl. Fract. Mech.*, **52**, 183-194.
- Berto, F. and Lazzarin, P. (2010), "Fictitious notch rounding approach of pointed V-notches under inplane shear", *Theor. Appl. Fract. Mech.*, **53**, 127-135
- Berto, F. and Zappalorto, M. (2011), "Fictitious notch rounding concept applied to V-notches with end holes under mode I loading", *Int. J. Fract.*, **171**, 91-98.
- Berto, F. (2012), "Fictitious notch rounding concept applied to V-notches with end holes under mode III loading", *Int. J. Fatigue*, **38**, 188-193.
- Berto, F. and Zappalorto, M. (2012), "The fictitious notch rounding approach applied to V-notches with root holes subjected to mode I loading", *J. Strain Anal.*, **47**(3), 176-186.
- Berto, F., Lazzarin, P. and Ayatollahi, M.R. (2012a), "Brittle fracture of sharp and blunt V-notches in isostatic graphite under torsion loading", *Carbon*, **50**, 1942-1952.
- Berto, F., Lazzarin, P. and Marangon, C. (2012b), "Brittle fracture of U-notched graphite plates under mixed mode loading", *Mater. Des.*, **41**, 421-432.
- Berto, F., Lazzarin, P. and Ayatollahi, M.R. (2013), "Brittle fracture of sharp and blunt V-notches in isostatic graphite under pure compression loading", *Carbon*, **63**, 101-116.
- Berto, F. and Lazzarin, P. (2014), "Recent developments in brittle and quasi-brittle failure assessment of engineering materials by means of local approaches", *Mater. Sci. Eng. R*, **75**, 1-48.
- Berto, F., Lazzarin, P. and Gallo, P. (2013), "High-temperature fatigue strength of a copper cobalt-beryllium alloy", *J. Strain Anal. Eng. Des.*, DOI: 10.1177/0309324713511804.
- Berto, F., Lazzarin, P., Harding, S. and Kotousov, A. (2012c), "Out-of-plane singular stress fields in V-notched plates and welded lap joints induced by in-plane shear load conditions", *Fat. Fract. Eng. Mater. Struct.*, **34**, 291-304.
- Berto, F., Lazzarin, P., Kotousov, A. and Pook, L. (2012c), "Induced out-of-plane mode at the tip of blunt lateral notches and holes under in-plane shear loading", *Fat. Fract. Eng. Mater. Struct.*, **35**, 538-555.
- Brighenti, R. (2008), "A new discontinuous FE formulation for crack path prediction in brittle solids", *Int. J. Solids Struct.*, **45**, 6501-6517.
- Brighenti, R. and Carpinteri, A. (2013a), "Surface cracks in fatigued structural components: A review", *Fat. Fract. Eng. Mater. Struct.*, **36**(12), 1209-1222.
- Bruno, A. and Latella, T.L. (2006), "The initiation and propagation of thermal shock cracks in graphite", *Carbon*, **44**, 3043-3048.
- Carpinteri, A., Brighenti, R. and Vantadori, S. (2010a), "Influence of the cold-drawing process on fatigue crack growth of a V-notched round bar", *Int. J. Fatigue*, **32**, 1136-1145.

- Carpinteri, A., Ronchei, C. and Vantadori, S. (2013), "Stress intensity factors and fatigue growth of surface cracks in notched shells and round bars: Two decades of research work", *Fat. Fract. Eng. Mater. Struct.*, **36**(11), 1164-1177.
- Carpinteri, A., Spagnoli, A. and Vantadori, S. (2010b), "A multifractal analysis of fatigue crack growth and its application to concrete", *Eng. Fract. Mech.*, **77**(6), 974-984.
- Etter, T., Kuebler, J., Frey, T., Schulz, P., Löffler, J.F. and Uggowitz, P.J. (2004), "Strength and fracture toughness of interpenetrating graphite/aluminum composites produced by the indirect squeeze casting process", *Mater. Sci. Eng. A*, **386**, 61-67.
- Glinka, G. (1985), "Energy density approach to calculation of inelastic strain stress near notches and cracks", *Eng. Fract. Mech.*, **22**(3), 485-508.
- Glinka, G., Shen, G. and Plumtree, A. (1995), "Multiaxial fatigue strain energy density parameter related to the critical fracture plane", *Fat. Fract. Eng. Mater. Struct.*, **18**(1), 37-46.
- Gómez, F.J., Elices, M., Berto, F. and Lazzarin, P. (2007), "Local strain energy to assess the static failure of U-notches in plates under mixed mode loading", *Int. J. Fract.*, **145**, 29-45.
- Harding, S., Kotousov, A., Lazzarin, P. and Berto, F. (2010), "Transverse singular effects in V-shaped notches stressed in mode II", *Int. J. Fract.*, **164**, 1-14.
- Jae, H.K., Young, S.L., Duck, H.K., No, S.P., Jeong, S.J., Kim, O. and Moon, S.I. (2004), "Evaluation of thermal shock strengths for graphite materials using a laser irradiation method", *Mater. Sci. Eng. A*, **387-389**, 385-389.
- Kawakami, H. (1985), "Notch sensitivity of graphite materials for VHTR", *J. Atom. Energy Soc. Jap.*, **27**(4), 357-364.
- Kotousov, A., Lazzarin, P., Berto, F. and Harding, S. (2010), "Effect of the thickness on elastic deformation and quasi-brittle fracture of plate components", *Eng. Fract. Mech.*, **77**, 1665-1681.
- Lazzarin, P., Berto, F. and Ayatollahi, M.R. (2013), "Brittle failure of inclined key-hole notches in isostatic graphite under in-plane mixed mode loading", *Fat. Fract. Eng. Mater. Struct.*, **36**(9), 942-955.
- Lazzarin, P. and Zambardi, R. (2001), "A finite-volume-energy based approach to predict the static and fatigue behavior of components with sharp V-shaped notches", *Int. J. Fract.*, **112**, 275-298.
- Lazzarin, P. and Berto, F. (2005), "Some expressions for the strain energy in a finite volume surrounding the root of blunt V-notches", *Int. J. Fract.*, **135**, 161-185.
- Lazzarin, P., Berto, F., Elices, M. and Gomez, F.J. (2009), "Brittle failures from U- and V-notches in mode I and mixed, I + II, mode: A synthesis based on the strain energy density averaged on finite-size volumes", *Fat. Fract. Eng. Mater. Struct.*, **32**(8), 671-684.
- Lazzarin, P., Berto, F., Gómez, F.J. and Zappalorto, M. (2008), "Some advantages derived from the use of the strain energy density over a control volume in fatigue strength assessments of welded joints", *Int. J. Fatigue*, **30**, 1345-1357.
- Lazzarin, P., Berto, F. and Zappalorto, M. (2010), "Rapid calculations of notch stress intensity factors based on averaged strain energy density from coarse meshes: Theoretical bases and applications", *Int. J. Fatigue*, **32**, 1559-1567.
- Lomakin, E.V., Zobnin, A.I. and Berezin, A.V. (1975), "Finding the fracture toughness characteristics of graphite materials in plane strain", *Strength Mater.*, **7**(4), 484-487.
- Mostafavi, M. and Marrow, T.J. (2012), "Quantitative in situ study of short crack propagation in polygranular graphite by digital image correlation", *Fat. Fract. Eng. Mater. Struct.*, **35**, 695-707.
- Mostafavi, M., McDonald, S.A., Çetinela, H., Mummery, P.M. and Marrow, T.J. (2013), "Flexural strength and defect behaviour of polygranular graphite under different states of stress", *Carbon*, **59**, 325-336.
- Nakhodchi, S., Smith, D.J. and Flewitt, P.E.J. (2013), "The formation of fracture process zones in polygranular graphite as a precursor to fracture", *J. Mater. Sci.*, **48**, 720-732.
- Neuber, H. (1958), *Theory of notch stresses*, Kerbspannungslehre, Springer-Verlag, Berlin, Germany.
- Radaj, D., Berto, F. and Lazzarin, P. (2009a), "Local fatigue strength parameters for welded joints based on strain energy density with inclusion of small-size notches", *Eng. Fract. Mech.*, **76**, 1109-1130.
- Radaj, D., Lazzarin, P. and Berto, F. (2009b), "Fatigue assessment of welded joints under slit-parallel loading based on strain energy density or notch rounding", *Int. J. Fatigue*, **31**, 1490-1504.

- Radaj, D., Lazzarin, P. and Berto, F. (2013), "Generalised Neuber concept of fictitious notch rounding", *Int. J. Fatigue*, **51**, 105-115.
- Sato, S., Kawamata, K., Awaji, H., Osawa, M. and Manaka, M. (1981), "Thermal shock resistance and fracture toughness during the graphitization process", *Carbon*, **19**, 111-118.
- Shi, L., Haiyan, L., Zhenmin, Z., Fok, A.S.L., Marsden, B.J., Hodgkins, A., Mummery, P.M. and Marrow, J. (2008), "Analysis of crack propagation in nuclear graphite using three-point bending of sandwiched specimens", *J. Nucl. Mater.*, **372**, 141-151.
- Sih, G.C. (1974), "Strain-energy-density factor applied to mixed mode crack problems", *Int. J. Fract.*, **10**, 305-321.
- Smith, D.J., Ayatollahi, M.R. and Pavier, M.J. (2001), "The role of T-stress in brittle fracture for linear elastic materials under mixed mode loading", *Fat. Fract. Eng. Mater. Struct.*, **24**(2), 137-150.
- Torabi, A.R. (2013a), "Fracture assessment of U-notched graphite plates under tension", *Int. J. Fract.*, **181**, 285-292.
- Torabi, A.R. (2013b), "Sudden fracture from U-notches in fine-grained isostatic graphite under mixed mode I/II loading", *Int. J. Fract.*, **181**, 309-316.
- Torabi, A.R., Fakoor, M. and Pirhadi, E. (2013a), "Tensile fracture in coarse-grained polycrystalline graphite weakened by a U-shaped notch", *Eng. Fract. Mech.*, **111**, 77-85.
- Torabi, A.R., Fakoor, M. and Darbani, M.A. (2013b), "Pure shear fracture study in a brittle graphite material containing a U-notch", *Int. J. Damage Mech.*, DOI: 10.1177/1056789513514071.
- Torabi, A.R., Fakoor, M. and Pirhadi, E. (2013c), "Fracture analysis of U-notched disc-type graphite specimens under mixed mode loading", *Int. J. Solids Struct.*, **51**(6), 1287-1298.
- Torabi, A.R. and Jafarinezhad, M.R., (2012), "Comprehensive data for rapid calculation of notch stress intensity factors in U-notched Brazilian disc specimen under tensile-shear loading", *Mater. Sci. Eng. A*, **541**, 135-142.
- Torabi, A.R. and Berto, F. (2013), "Strain energy density to assess mode II fracture in U-notched disk-type graphite plates", *Int. J. Damage Mech.*, DOI: 10.1177/1056789513519349.
- Yamauchi, Y., Nakano, M., Kishida, K. and Okabe, T. (2001), "Measurement of mixed-mode fracture toughness for brittle materials using edge-notched half-disk specimen", *Zairyo/J. Soc. Mater. Sci. Jap.*, **50**, 224-229.
- Yosibash, Z., Bussiba, A. and Gilad, I. (2004), "Failure criteria for brittle elastic materials", *Int. J. Fract.*, **125**, 307-333.